Eur Biophys J (1999) 28: 605–609

BIOPHYSICS LETTER

Steffen Michalek · Holger Lerche · Mirko Wagner
Nenad Mitrović · Michael Schiebe
Frank Lehmann-Horn · Jens Timmer

On identification of Na^+ channel gating schemes using moving-average filtered hidden Markov models

Received: 11 February 1999 / Revised version: 18 June 1999 / Accepted: 21 June 1999

Abstract Transitions between distinct kinetic states of an ion channel are described by a Markov process. Hidden Markov models (HMM) have been successfully applied in the analysis of single ion channel recordings with a small signal-to-noise ratio. However, we have recently shown that the anti-aliasing low-pass filter misleads parameter estimation. Here, we show for the case of a Na^+ channel recording that the standard HMM do neither allow parameter estimation nor a correct identification of the gating scheme. In particular, the number of closed and open states is determined incorrectly, whereas a modified HMM considering the anti-aliasing filter (moving-average filtered HMM) is able to reproduce the characteristic properties of the time series and to perform gating scheme identification.

Key words Single channel recording · Sodium channel · Gating scheme · Hidden Markov model · Anti-aliasing filter

Introduction

Gating mechanisms of ion channels can be investigated using Markov models (Horn and Lange 1983; Horn and Vandenberg 1984; Horn et al. 1984; Vandenberg and Bezanilla 1991) if the signal-to-noise ratio is large enough to obtain idealized records (Colquhoun and Hawkes 1995; Colquhoun and Sigworth 1995). Hidden Markov models (HMM) have been successfully applied in the analysis of single-channel recordings with a smaller signal-to-noise ratio (Chung et al. 1990; Fredkin and Rice 1992; Becker et al. 1994). Their concept assumes instantaneous transitions without memory as well as uncorrelated noise. However, the data generating physical system often causes substantial violation of those idealizing assumptions, namely additional correlations within the amplified signal (the power increases with frequency; Sigworth 1995) and correlations due to the necessity of anti-aliasing filtering before digital sampling. On the basis of computer simulations, the standard (unfiltered) HMM has been shown to be inadequate for estimating rate constants in filtered signals (Venkataramanan et al. 1998; Michalek et al. 1999). We recently developed a method to incorporate filtering into the analysis, the moving-average filtered HMM (MA-filtered HMM), and showed that this method provides unbiased estimators (Michalek et al. 1999).

Our interest is characterizing the functional behavior of human muscle Na^+ channels by means of dynamic models. Here, we compare the analysis of a single channel measurement by both unfiltered HMM and MA-filtered HMM. Whereas the unfiltered HMM is severely affected by filtering, the MA-filtered HMM provides an identification of the gating scheme that is reproducible in computer simulations.

Materials and methods

Single channel measurements

Recordings of single Na^+ channels were performed using a human embryonic kidney cell line (HEK-293) stably expressing F1473S mutant Na^+ channels (Fleischhauer et al. 1998). We used an EPC-7 amplifier (List, Darmstadt, Germany) and pClamp 6.02 data acquisition (Axon instruments, Foster City, Calif., USA). Data were low-pass filtered at 10 kHz with a 4-pole

S. Michalek · M. Wagner · J. Timmer (✉)
FDM – Center for Data Analysis, University of Freiburg, Eckerstrasse 1, D-79104 Freiburg im Breisgau, Germany
e-mail: jens.timmer@fdm.uni-freiburg.de

H. Lerche · N. Mitrović · M. Schiebe · F. Lehmann-Horn
Department of Applied Physiology, University of Ulm, Germany

Bessel filter of the amplifier and a second analog 8-pole Bessel filter (Zeitz, Augsburg, Germany), and were sampled at 50 kHz. Digitized data were transferred to Sparc Ultra workstations (Sun Microsystems) and also to an Origin 2000 computer (Silicon Graphics). Cell-attached patches were held at −120 mV and depolarized to −20 mV for 20 ms. Two thousand consecutive traces were recorded at room temperature (21–22 °C). Leakage and capacitative currents were eliminated by subtracting averaged and scaled records without channel activity. The number of channels in a patch was determined by inspecting traces and counting the maximum number of channels that open simultaneously (Horn 1991). The first 3 ms of the first 600 traces of the best recording containing a single Na^+ channel were taken for evaluation. Raw data are shown in Fig. 1a.

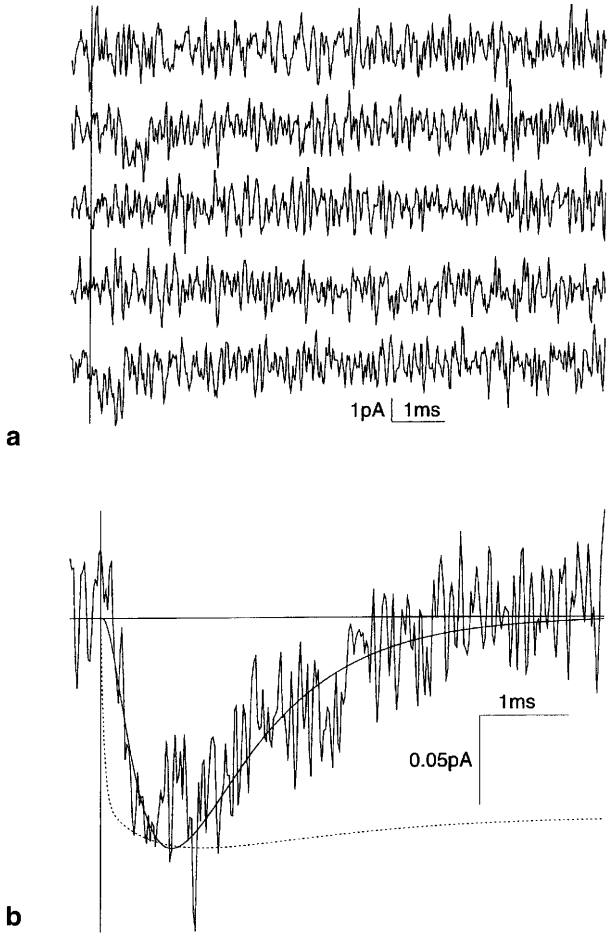

Fig. 1 **a** Representative raw current traces of single channel recordings. Openings (plotted downwards) occur in traces 2 and 5. **b** Theoretical time course of the average current from the filtered HMM (*solid*, *smooth*) and from the unfiltered HMM (*dotted*) for comparison with the average over the 600 recorded traces (*vertical line* at start of depolarization). The theoretical curves are scaled for equal peak height by a scaling factor of 0.7 (filtered HMM) and of 0.63 (unfiltered HMM)

Theory

HMM and MA(q,b)-filtered HMM

The unfiltered/filtered HMM

A HMM assumes as the data generating process the stochastic transitions between a finite set of states, which represent classes of molecular conformations with a certain conductivity. These jumps are instantaneous, following a homogeneous continuous-time Markov process which is given by the transition rates in a so-called gating scheme defining the directed graph of allowed transitions between the states. This so-called background process $\boldsymbol{X} = (X_t)_{0 \le t < N}$ is hidden under white noise. By discrete sampling, the observed unfiltered time series $\boldsymbol{Y} = (Y_t)_{0 \le t < N}$ is obtained:

$$Y_t = \mu(X_t) + \sigma(X_t)\epsilon_t \tag{1}$$

with expectation value μ, standard deviation σ, and i.i.d. random variables $\epsilon_t \sim \mathcal{N}(0,1)$.

Correlated noise as well as finite impulse response filters can be taken into account by regarding the MA(q,b)-filtered HMM with observed process $\boldsymbol{Z} = (\mathrm{Z}_t)_{0 \le t < N}$

$$\begin{aligned} Z_t &= \sum_{l=0}^{b} \chi_l \, \mu(X_{t-l}) + \eta_t \\ \eta_t &= \sum_{m=0}^{q} \vartheta_m \, \sigma(X_{t-m})\epsilon_{t-m} \end{aligned} \tag{2}$$

where $\chi_0, \ldots, \chi_b$ and $\vartheta_0, \ldots, \vartheta_q$ are the filter coefficients for filtering the background process and the noise, respectively.

General auto-regressive moving-average (ARMA) filtered HMM are described in (Michalek et al. 1999). The concept of discretely sampled continuous-time HMM is discussed in Michalek and Timmer (1999).

Parameter estimation and gating scheme identification with unfiltered/filtered HMM

Parameters in unfiltered HMM can be obtained by maximum likelihood estimators (Fredkin and Rice 1992; Albertsen and Hansen 1994; Qin et al. 1997; Michalek and Timmer 1999). For filtered HMM, the approximate likelihood estimator has been shown to be unbiased in computer simulations of the same type as the present ion channel recordings (Michalek et al. 1999). Comparison between different gating schemes incorporating different numbers of states or different graphs of allowed transitions can be performed by means of the likelihood ratio test (LRT) as in the case of Markov models (Kienker 1990): for nested models with parameter spaces $\Theta_{\text{small}} \subset \Theta_{\text{big}}$, $r := \dim \Theta_{\text{big}} - \dim \Theta_{\text{small}} > 0$, and the true parameter ϑ_0 lying in the interior of Θ_{small}, twice the difference of the log-likelihoods is χ^2_r distributed. If ϑ_0 is

on the border of Θ_{small}, a test based on this distribution is conservative (Wagner et al. 1999).

Results and discussion

Gating scheme identification using unfiltered/filtered HMM

Gating schemes for the Na^+ channel

A simple model that has often been used in the past to calculate rate constants contains one open, one inactivated, and several closed states (Horn and Lange 1983; Horn and Vandenberg 1984; Patlak 1991; Chahine et al. 1994):

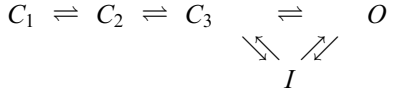

Here, C, O and I denote closed, open and inactivated states, respectively. Of course, not all of the possible transitions within this gating scheme contribute to the statistical properties of finite measurements in such a way that they are necessary to describe the time series. In the following, we want to decide which gating scheme performs the best description in a statistical sense: a more complex scheme is only preferred to a simpler one if the respective LRT rejects the null hypothesis that the simpler scheme fits equally well.

Table 1 shows those fitted gating schemes that contribute to the decisions. The values of the log-likelihood were obtained using unfiltered HMM and MA(2,2)-filtered HMM following Eq. (2), respectively. The MA(2,2)-filtered HMM was recently shown to be of adequate order for the present type of ion channel recordings (Michalek et al. 1999). The initial probability of the Markov process was always equal to 1 for the outmost left closed state C or C_1. States C_n and I were costrained to have identical output levels and output noise variances within each model, and the same was forced for open states O_n (parametrization techniques can be found in Klein et al. 1997; Michalek and Timmer 1999; Michalek et al. 1999).

Gating scheme identification using unfiltered HMM

The gating scheme identification by LRT in the unfiltered case clearly yields the following result, where $A \rightarrow B$ denotes a decision towards B:

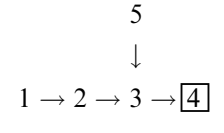

We start with the simplest model 1. The LRT against model 2 rejects the null hypothesis that they fit equally to the measurement: as expected, an inactivated state is necessary. The subsequent tests yield: model 3 is preferred to model 2, model 5 is not preferred to model 3, while finally model 4 is preferred to model 3. (Model 5 always estimates a very high rate for $C_1 \rightarrow C_2$, and rate zero for the opposite direction. The fitting procedure never finishes with increasing the rate constant, and the log-likelihood result therefore is little lower than that of model 3.)

We conclude that application of the unfiltered HMM to this measurement would argue strongly for the existence of (at least) two open states. Concerning the number of initially passed closed states, there is no necessity to assume more than one initial closed state in order to characterize the present time series.

Table 1 Log-likelihood values for different gating schemes, obtained by unfiltered and MA(2,2)-filtered HMM. Only those values are given which contribute to the identification decision

Gating scheme No.	Transition Graph	Log-likelihood	
		HMM	MA-HMM
1		−83068.54	−52493.15
2		−82974.02	−52480.13
3	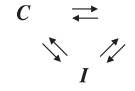	−82900.25	−52383.45
4	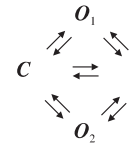	−82272.96	–
5	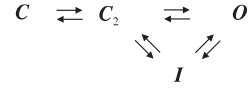	−82900.32	−52366.32
6	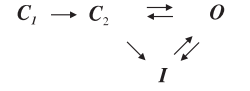	–	−52366.32
7	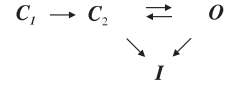	–	−52367.04
8	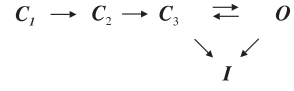	–	−52367.99
9	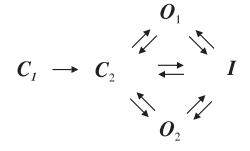	–	−52364.33

Gating scheme identification using MA(q,b)-filtered HMM

The gating scheme identification based on MA(2,2)-filtered HMM yields the following result when starting

with model 1 and subsequent testing for models of different complexity:

$$1 \rightarrow 2 \rightarrow 3 \rightarrow 5 \rightarrow 6 \rightarrow \boxed{7} \begin{array}{l} \uparrow 8 \\ \downarrow 9 \end{array}$$

Two details about these tests should be mentioned. (1) Model 8 always estimates a very high rate $C_1 \rightarrow C_2$, so that the fitting procedure never finishes properly, and the obtained log-likelihood therefore is little lower than that of model 7. (2) The fit of model 9 yields three rates estimated to zero, indicating a smaller number of degrees of freedom (8 instead of 11), but this does not affect the decision in the present case, where twice the difference of the log-likelihoods of models 7 and 9 is about 5.4. For comparison, the 95% quantile of the χ^2_3 distribution is 5.99. So, there is no reason to reject the null hypothesis that a model with two open states does not provide a better description of the measurement.

Since the Markov dynamics starts in C_1, any model containing two directly connected open states accessible from either C_2 or I in model 9 is statistically equivalent to model 9, where the two open states are separated (Kienker 1990). Hence, we conclude that the present data set does not give evidence for the presence of two different open states in the Na^+ channel, as has been described previously (Horn and Vandenberg 1984). At least, the present experimental and measurement setting does not show a significant contribution of a second open state. However, a second open state may contribute under different experimental situations, as has been observed when analyzing bursts of channel reopenings (Mitrović et al. 1994; Lerche et al. 1996). The number of initially passed closed states that are necessary for a description of the measurement appears to be at least two, indicating that the so-called first latency is caused by a time consuming multi-step process, as has been observed previously (Horn et al. 1984).

Reproducibility of the average time course

The theoretical average time course was calculated from the rate constants of the best model for both the unfiltered and the MA-filtered HMM. Superposition of the theoretical curves to the raw data is shown in Fig. 1b. The prediction of model 7 derived from the filtered HMM fits well to the activation and inactivation kinetics of the raw data average. However, it overestimates the overall open probability by 30%. The fit of model 4 from the unfiltered HMM does not reproduce the current time course. A possible explanation could be that an unfiltered model interpreting the correlated noise as changes between states while ignoring the activation and inactivation dynamics does fit better to the overall correlation structure than an unfiltered model regarding channel openings and closings.

Table 2 Fitted parameters for model 7 on both the measurement and the simulated data set obtained by means of the MA(2,2)-filtered and the standard HMM, respectively. Each model behaves very similar on the measurement and on the simulation. It was not possible to obtain estimation errors for the unfiltered HMM, since the Hessian of the log-likelihood is singular for this model

Transition rate in model 7	Fitted values (s^{-1})			
	MA(2,2)-HMM		Unfiltered HMM	
	Data set	Simulation	Data set	Simulation
$C_1 \rightarrow C_2$	3400 ± 900	2800 ± 500	$>4 \times 10^5$	$>2 \times 10^5$
$C_2 \rightarrow O$	1500 ± 500	1800 ± 500	2500	2700
$C_2 \rightarrow I$	3200 ± 1100	3900 ± 1100	310	2
$O \rightarrow C_2$	430 ± 230	560 ± 230	9013	9500
$O \rightarrow$ I	730 ± 180	720 ± 190	0	4

Consistency of the MA(2,2)-filtered HMM

We simulated 600 traces, each with a length of 3 ms, of 50 kHz sampled ion channel data using gating scheme, rate constants, and conductivity levels from the best fit model 7. The standard deviation of the white noise before filtering had to be increased for the simulation in order to obtain a comparable noise level after filtering. The simulation was done with 10-times oversampling in order to obtain a quasi-analog time series. The data were then digitally filtered using the transfer function of an 8-pole Bessel filter with 3-dB cut-off frequency at 10 kHz (i.e. $0.02 \times \Delta t^{-1}$ in units of the oversampled time series), and afterwards down-sampled by a factor of 10. This processing reflects the data generating process assuming the low-pass filter as the main source of additional correlations violating the model's assumptions.

Table 2 shows the fitted parameters on the original data as well as on the simulated data set for both the MA(2,2)-filtered HMM and the unfiltered HMM. The proper reproduction of the simulating parameters indicates that a data generating process following model 7 can be identified reliably from a respective realization when using MA(2,2)-filtered HMM.

Fitting model 9 to the simulated data yields a twofold log-likelihood difference of 0.35 when compared with model 7. Thus, the correct number of open states can be determined.

Artifacts when using unfiltered HMM

On the simulated data set, it is not possible to reproduce the correct rate constants when using the standard HMM. The character of the results obtained by the unfiltered HMM is the same for the measured and for the simulated data (see Table 2). Also, a LRT comparing models 3 and 4 by means of a standard HMM as for

the measurement again strongly requires a second open state; twice the difference of the log-likelihood values again exceeds 600.

We conclude that both the parameter estimation and the gating scheme identification obtained by means of the unfiltered HMM when analyzing the simulated data set can be understood as a misinterpretation caused by not considering the low-pass filter. Furthermore, the results when analyzing the present measurement by means of unfiltered HMM show a very similar behavior as in the case of the simulations. So, they can be understood as filter artifacts, too.

Conclusions

The gating scheme identification is clearly distinct when using either unfiltered or MA-filtered HMM. The number of contributing initially passed closed states as well as the number of open states is determined differently. We conclude that for determination of the adequate gating scheme the additional effort of the MA-filtered HMM is necessary, since gating scheme identification using standard HMM yields misinterpretations whereas the MA-filtered HMM is able to reproduce the dynamics of the data set. The different result when using standard HMM can be understood as an artifact induced by low-pass filtering. We should mention that the correct mean open time is as long as 43 sample intervals, here. However, the analysis is disturbed severely when using the unfiltered HMM, although the response time of the low-pass filter is less than 4 intervals.

By means of MA-filtered HMM as a new instrument, further investigations will be concerned with the differences in the functional behavior of wild-type and mutant Na^+ channels.

Acknowledgements We thank Dr. R. Horn for helpful comments on this manuscript. This work was supported by the Deutsche Forschungsgemeinschaft (DFG Ho 496/4-2, DFG Le 481/3-3).

References

Albertsen A, Hansen U-P (1994) Estimation of kinetic rate constants from multi-channel recordings by a direct fit of the time series. Biophys J 67: 1393–1403

Becker J, Honerkamp J, Hirsch J, Schlatter E, Greger R (1994) Analyzing ion channels with hidden Markov models. Pflügers Arch 426: 328–332

Chahine M, George AL, Zhou M, Ji S, Sun W, Barchi RL, Horn R (1994) Sodium channel mutations in paramyotonia congenita uncouple inactivation from activation. Neuron 12: 281–294

Chung S-H, Moore J, Xia L, Premkumar LS, Gage PW (1990) Characterization of single channel currents using digital signal processing techniques based on hidden Markov models. Phil Trans R Soc Lond Ser B 329: 265–285

Colquhoun D, Hawkes AG (1995) The principles of the stochastic interpretation of ion-channel mechanisms. In: Sakmann B, Neher E (eds) Single-channel recording, 2nd edn. Plenum Press, New York, pp 397–482

Colquhoun D, Sigworth FJ (1995) Fitting and statistical analysis of single-channel records. In: Sakmann B, Neher E (eds) Single-channel recording, 2nd edn. Plenum Press, New York, pp 483–587

Fleischhauer R, Mitrović N, Deymeer F, George AL, Lehmann-Horn F, Lerche H (1998) Effects of temperature and mexiletine on a sodium channel mutation causing paramyotonia congenita. Pflügers Arch 436: 757–765

Fredkin D, Rice J (1992) Maximum likelihood estimation and identification directly from single-channel recordings. Proc R Soc Lond Ser B 249: 125–132

Horn R (1991) Estimating the number of channels in patch recordings. Biophys J 50: 433–439

Horn R, Lange K (1983) Estimating kinetic constants from single channel data. Biophys J 43: 207–223

Horn R, Vandenberg C (1984) Statistical properties of single sodium channels. J Gen Physiol 84: 505–534

Horn R, Vandenberg C, Lange K (1984) Statistical analysis of single sodium channels. Biophys J 45: 323–35

Kienker P (1990) Equivalence of aggregated Markov models of ion-channel gating. Proc R Soc Lond Ser B 236: 269–309

Klein S, Timmer J, Honerkamp J (1997) Analysis of multichannel patch clamp recordings by hidden Markov models. Biometrics 53: 870–884

Lerche H, Mitrović N, Dubowitz V, Lehmann-Horn F (1996) Paramyotonia congenita: the R1448P Na^+ channel mutation in adult human skeletal muscle. Ann Neurol 39: 599–608

Michalek S, Timmer J (1999) Estimating rate constants in hidden Markov models by the EM algorithm. IEEE Trans Sig Proc 47: 226–228

Michalek S, Wagner M, Timmer J (1999) A new approximate likelihood estimator for ARMA-filtered hidden Markov models. IEEE Trans Sig Proc 47 (in press)

Mitrović N, George AL, Heine R, Wagner S, Pika U, Hartlaub U, Zhou M, Lerche H, Fahlke C, Lehmann-Horn F (1994) K^+-aggravated myotonia: destabilization of the inactivated state of the human muscle Na^+ channel by the V1589M mutation. J Physiol 478: 395–402

Patlak J (1991) Molecular kinetics of voltage-dependent Na^+ channels. Physiol Rev 71: 1047–80

Qin F, Auerbach A, Sachs F (1997) Maximum likelihood estimation of aggregated Markov processes. Proc R Lond Ser Soc B 264: 375–383

Sigworth FJ (1995) Electronic design of the patch clamp. In: Sakmann B, Neher E (eds) Single-channel recording, 2nd edn. Plenum Press, New York, pp 95–127

Vandenberg CA, Bezanilla F (1991) A sodium channel gating model based on single channel, macroscopic ionic, and gating currents in the squid giant axon. Biophys J 60: 1511–1533

Venkataramanan L, Walsh JL, Kuc R, Sigworth F (1998) Identification of hidden Markov models for ion channel currents, part I: colored, background noise. IEEE Trans Sig Proc 46: 1901–1915

Wagner M, Michalek S, Timmer J (1999) Testing for the number of states in hidden Markov models with application to ion channel data. In: Gaul W, Locarek-Junge H (eds) Studies in classification, data analysis, and knowledge organization. Springer, Berlin Heidelberg New York, pp 260–267